

Faraday Discussions

Accepted Manuscript



This manuscript will be presented and discussed at a forthcoming Faraday Discussion meeting. All delegates can contribute to the discussion which will be included in the final volume.

Register now to attend! Full details of all upcoming meetings: <http://rsc.li/fd-upcoming-meetings>



This is an *Accepted Manuscript*, which has been through the Royal Society of Chemistry peer review process and has been accepted for publication.

Accepted Manuscripts are published online shortly after acceptance, before technical editing, formatting and proof reading. Using this free service, authors can make their results available to the community, in citable form, before we publish the edited article. We will replace this *Accepted Manuscript* with the edited and formatted *Advance Article* as soon as it is available.

You can find more information about *Accepted Manuscripts* in the [Information for Authors](#).

Please note that technical editing may introduce minor changes to the text and/or graphics, which may alter content. The journal's standard [Terms & Conditions](#) and the [Ethical guidelines](#) still apply. In no event shall the Royal Society of Chemistry be held responsible for any errors or omissions in this *Accepted Manuscript* or any consequences arising from the use of any information it contains.

Localizing and inducing primary nucleation

Zoubida Hammadi¹, Romain Grossier¹, Aziza Ikni², Nadine Candoni¹, Roger Morin¹, Stéphane Veessler¹

¹CINaM-CNRS, Aix-Marseille Université, Campus de Luminy F-13288 Marseille, France

²SPMS-CNRS, UMR 8580, Grande Voie des Vignes, F-92295 Châtenay-Malabry, France

Abstract

Do the differing properties of materials influence their nucleation mechanisms? We present different experimental approaches to study and control nucleation, and shed light on some of the factors affecting the nucleation process.

Introduction

The control of material properties being directly related to their methods of production, understanding the mechanisms governing these methods is vital. With crystallized materials, such as minerals, pharmaceuticals, proteins, biominerals, nanomaterials, the most important properties, crystal morphology, habit, size distribution and phases, are controlled by the nucleation step. Nucleation was clearly defined by D. Kashchiev: “it is the process of random generation of those nanoscopically small formations of the new phase that have the ability for irreversible overgrowth to macroscopic sizes.”¹ The size of critical cluster and the nucleation rate are determined by the classical nucleation theory (CNT) derived from the Gibbs treatment of droplet nucleation.² Interestingly, this simple model fits experimental results very well but is many orders of magnitude out in predicting nucleation frequencies, as shown on protein crystallization.³ It is noteworthy that even experimental data on the same system in the same conditions can have discrepancies of more than 10 orders of magnitude³⁻⁷ as illustrated in Figure 1.

Moreover, in several studies on protein crystallization using solution scattering techniques, ultracentrifugation-sedimentation and dialysis kinetics, data were interpreted as indicating the formation of prenucleation aggregates, clusters or oligomeric species, ranging between monomer and crystal.⁸⁻¹⁹ But other authors²⁰⁻²⁶ did not observe such aggregates and offered the following explanation: “the failure to account for direct and indirect protein interactions in the solutions results in unrealistic aggregation scenarios”.²³ Note that the stable entity in solution is not necessarily a monomer; it can be an oligomer, for biological or physicochemical reasons.²⁷ Finally, simulation papers published in the same period proposed a 2-step process for protein crystal nucleation²⁸⁻³⁰ using the presence of a metastable LLPS (liquid liquid phase separation) to reduce the nucleation free-energy barrier. The first step could be a local densification (liquid-like dense phase) and the second step could be the nucleation of the solid inside this dense phase. There has even been a third nucleation pathway proposed linked to biomineralization, consisting of a nucleation via stable prenucleation clusters.³¹

To summarize, in the CNT only one order parameter, density, describes the transition between the two phases, whereas in the 2-step theory two order parameters, density and structure are used. For reviews see.^{32, 33} This appears to us as an attempt to find a universally applicable explanation for experimental discrepancies. First, the limiting step, densification or

structuration, will depend on the solute, as suggested by Knezic et al.³⁴ for example, macromolecules take longer to rearrange themselves into crystalline nuclei than smaller molecules. Second, the fact that the location, the nature and the lifetime of the dense phase and/or the critical nucleus are unknown (at the moment) explains difficulties encountered in experimental observations and interpretations. In this paper, however, we explore nucleation from a purely practical point of view, without any a priori assumption on the nucleation mechanism. We describe the two experimental approaches taking here: indirect experiments measuring nucleation frequency by counting crystals or by measuring induction time, and direct experiments observing the critical nucleus. Kinetic measurements will provide us with data to be tested by classical and 2-step nucleation models³⁵. Whereas direct observation will give information on the size and structure of the critical nucleus. The objective is to unravel nucleation mechanisms in solution.

Experimental

Microfluidic set-up (~nL). Experiments were performed in PDMS (poly(dimethylsiloxane)) and PEEK (polyether ether ketone) and Teflon devices based on HPLC techniques, T-shaped junctions as described previously^{36, 37} or cross-shaped (Zhang et al submitted) ("plug-factory") were used to form the droplets with volumes in the nanoliter range, without addition of surfactants. We used FMS oil (Hampton Research) for aqueous solvents. This oil shows no or very low miscibility with water and good wettability with PDMS and Teflon. The droplet concentration and composition were varied using a programmable multi-channel syringe pump (neMESYS) and controlling the relative and absolute flow rates of the different solutions. (Zhang et al submitted) The tubing containing the droplets was placed in a thermostatted tubing-holder and incubated to obtain crystallization. Droplets were observed using an XYZ-motorized camera.

Production of microdroplets with microinjectors (~pL to fL). We used a simply-constructed and easy-to-use fluidic device that generates arrayed aqueous phase microdroplets in oil with volumes ranging from nanoliter to femtoliter, without addition of surfactant.³⁸ The device enables the entire volume range to be attained in the course of one experiment. All experiments were performed on a hydrophobic coverslip, at 20°C in a thermostatted room. The coverslip was covered with approximately 100µL of inert DMS oil (Hampton Research HR3-419, refractive index=1.390). The micrometer-sized droplets of water solution were generated on the coverslip by a microinjector (Femtojet Eppendorf) with a micropipette of 0.5µm internal diameter (Femtotip Eppendorf). Two home-made micromanipulators (MS30 Mechanics) consisting of 3 miniature translation stages allowed displacement of the injector (capillary holder) and the tip in X, Y and Z with a displacement of 18mm in the 3 directions by steps of 16nm. Here, we made the sharp tips from tungsten (W) wires (125µm diameter); for a detailed description see³⁹⁻⁴¹.

Localized DC electric field. The experimental set-up was composed of a crystallization cell with two electrodes at least one of which had a sharp W-tip, as previously described⁴¹. Two home-made micromanipulators allowing displacement of the electrodes in X, Y and Z were added.

Protein solutions. Hen-egg white lysozyme (14600Da, pI = 11.2) was purchased from Sigma (batch 057K7013 L 2879) and used without further purification. The purity of lysozyme was checked by molecular sieving. Proper amounts of Lysozyme and NaCl were dissolved in pure water (ELGA UHQ reverse osmosis system) to obtain the necessary stock solutions. The different solutions were buffered with 80mM acetic acid, adjusted to pH=4.5 with NaOH (1M) and filtered through 0.22µm Millipore filters. pH was checked with a pHmeter (Schott

Instrument, Prolab 1000) equipped with a pH microelectrode. Lysozyme concentrations were checked by optical density measurements (Shimadzu, UV-1800) using an extinction coefficient of $2.64 \text{ mL}\cdot\text{cm}^{-1}\cdot\text{mg}^{-1}$ at 280nm for lysozyme.

Gel solutions. A stock solution of 1% agarose type V from Sigma (gel point 42°C) was prepared using the method developed by Robert and Lefaucheu.⁴² Gel lysozyme solutions were prepared by mixing at 42°C the solutions of agarose gel, sodium chloride and protein yielding a final agarose concentration of 1% w/v. The mixture gelled in a few minutes once temperature was decreased.

Mineral solutions. NaCl (R.P. normapur, analytical reagent) solutions were prepared by dissolution of the proper amount of powder in pure water.

Oils. Dodecanemethylpentasiloxane (DMS) oil (Hampton Research HR2-593, refractive index=1.390 at 20°C) and paraffin oil (Hampton Research HR3-421, refractive index=1.467) were used as continuous phases.

Results and discussions

I. Indirect Experiments

The indirect measurement of nucleation is obtained through nucleation frequencies or induction times. Because nucleation is of a stochastic nature, it is important to perform a large number of experiments in order to obtain reliable data. Here nucleation was performed in small volumes in order to reduce the number of crystals and to render their observation easier. Moreover, this has the advantage of decreasing the quantity of molecules while speeding up heat and mass transfer.⁴³ In addition, the supersaturation range experimentally accessible is increased for kinetic⁴⁴ and thermodynamic⁴⁵ reasons. One kinetic limitation in small volumes arises from nucleation frequency (J/number of nucleus by unit time and volume): the smaller the volume, the longer the induction time and the wider the metastable zone, thus requiring greater supersaturation for nucleation^{46, 47}.

I.1. Small volumes of μL to nL range, the kinetic effect.

Our experiments used microfluidics technologies. Microfluidics has proved an efficient way of measuring nucleation frequency by measuring the probability of crystal presence in the droplets as a function of time⁴⁸⁻⁵⁰ and by counting the number of crystal nuclei per droplet.^{4, 44} Figure 1 summarizes data from different studies obtained using the double pulse technique.^{6, 51, 52} This technique allows direct determination of the steady-state rate of primary nucleation, separating crystal nucleation from the growth process, by counting nucleated crystals instead of estimating induction times. The discrepancies between data presented in Fig. 1 chiefly stem from the experimental method applied, where the supersaturation during the quench is not constant, according to the authors⁴. Note the agreement between data obtained in microbatches⁷ ($\sim 1\mu\text{L}$) and microfluidics⁴⁴ ($\sim 100\text{nL}$). When the volume is diminished, the range of experimentally measurable J is increased. One of the limitations usually involved in measuring J is the supersaturation range over which the experiment can be performed. When β is too low, nucleation frequency is low and nucleation is sensitive to local heterogeneity. When β is too high, J is difficult to measure because it is too rapid. This is why in practice, we are able to measure the nucleation frequency only in the vicinity of the metastable zone limit.

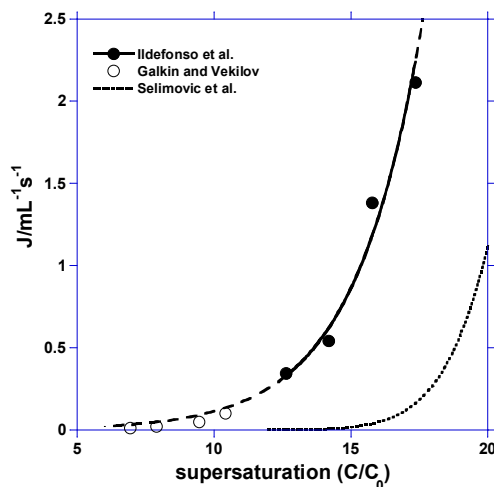


Fig. 1: Primary nucleation rate of lysozyme vs supersaturation, (●) data at 20°C- $C_0=3.2\text{mg/mL}$ ($\text{NaCl}=0.7\text{M}$ and $\text{pH}=4.5$) from Ildefonso et al. in microfluidics⁴⁴, (○) data, at 12.6°C- $C_0=1.6\text{mg/mL}$ ($\text{NaCl}=0.7\text{M}$ and $\text{pH}=4.5$), from Galkin and Vekilov in microbatches in oil⁷ and (...) data at 12°C- $C_0=5\text{mg/mL}$ ($\text{NaCl}=0.6\text{M}$ and $\text{pH}=4.5$) from Selimovic et al. in microfluidics.⁴

1.2. Small volumes of pL range, the thermodynamic effect.

Emulsion-based methods such as microfluidics have advantages; permitting production, storage and observation of a large number of microdroplets of controlled chemical composition, for instance. But microfluidics has also drawbacks: microdroplet size is controlled by channel size and microdroplets are not accessible (hardware limitation). Microdroplet generation with micropipets or microinjectors render microdroplets accessible and makes the size range easy to control. However, its drawback is that a single microdroplet is produced.^{43, 53, 54} Consequently, we recently presented a fluidic device³⁸ that generates arrayed aqueous phase microdroplets under oil (sessile geometry). This set-up combines the advantage of channelled microfluidic techniques, generating thousands of droplets (Fig. 2) with the advantage of micropipette techniques, control over size and microdroplet accessibility.

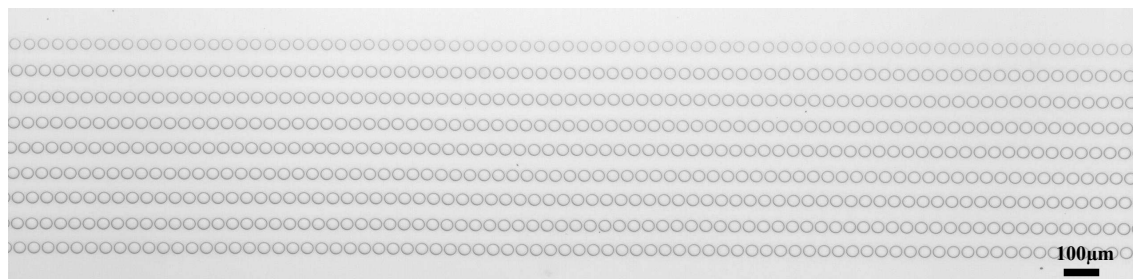


Fig. 2: Array of droplets (~720) of NaCl solutions generated through the layer of inert DMS oil.

As pointed out by Bempah and Hileman⁵⁵, “One major problem associated with the use of the droplet technique in nucleation studies is the creation of sufficient supersaturation within each droplet to ensure crystallization”. In other words the smaller the volume, the longer the

induction time and the wider the metastable zone. Hence a thermodynamic limitation appears because, contrary to the CNT which supposes an infinite reservoir of molecules, supersaturation is no longer constant during the nucleation process (aggregation of molecules) but is decreasing.⁴⁵ In these small-volume systems unexpected high-supersaturated metastable solutions are observed. In practice, there is an influence of volume on nucleation from picoliter range down.⁴⁵ This is in agreement with experimental results showing effects under nanoscopic confinement.⁵⁶⁻⁶⁰

We, therefore, used the droplet contraction method to generate sufficient supersaturation, i.e. diffusion of water from the microdroplet into the oil. The experiment presented in Figs.3 and 4 is isothermal (20°C) and volume is decreasing linearly⁶¹ with time and can be monitored throughout the experiment. In the first stage (Fig. 3), 3 microdroplet rows containing NaCl solution at $\beta=0.1$ are generated, and supersaturation β is defined as the ratio of the NaCl concentration in solution versus the solubility of NaCl, 6.15 M at 20°C in water.⁶² Droplets slowly evaporate until critical supersaturation is reached. The critical supersaturation for nucleation is the maximum supersaturation that a solution can withstand without nucleating a new phase.⁴⁷ The nucleation times of the microdroplets from the experiment (Figs.3 and 4) are plotted in Fig.5, $P(t)$ represents the normalized fraction of nucleated microdroplets. Due to the fast growth rate, the time required for the newly-formed nuclei to grow to a detectable size is negligible with regard to the induction time (see Fig.6). Thus, the time when a detectable crystal is observed can be considered the induction time. In the experiment shown in Figs.3 and 4, we observe that the smaller the volume the faster the evaporation rate and the faster the nucleation (Fig.5).

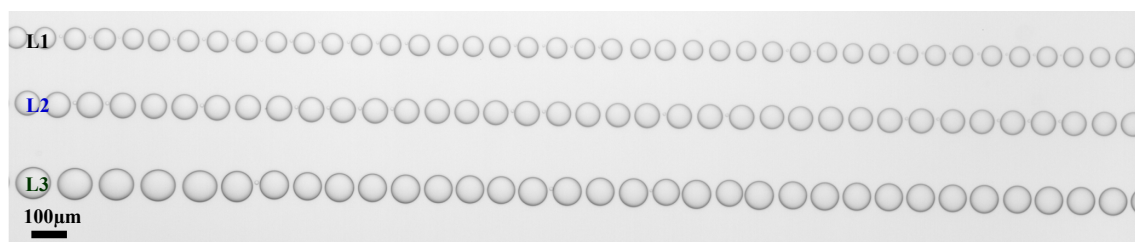


Fig. 3: Array of droplets of NaCl solutions at $\beta=0.1$ generated through the layer of inert DMS oil. Microdroplet volumes are 104, 172 and 284pL for rows L1, L2 and L3 respectively, 104pL assuming a spherical shape for the droplet with a contact angle of 130° as measured previously.⁶¹

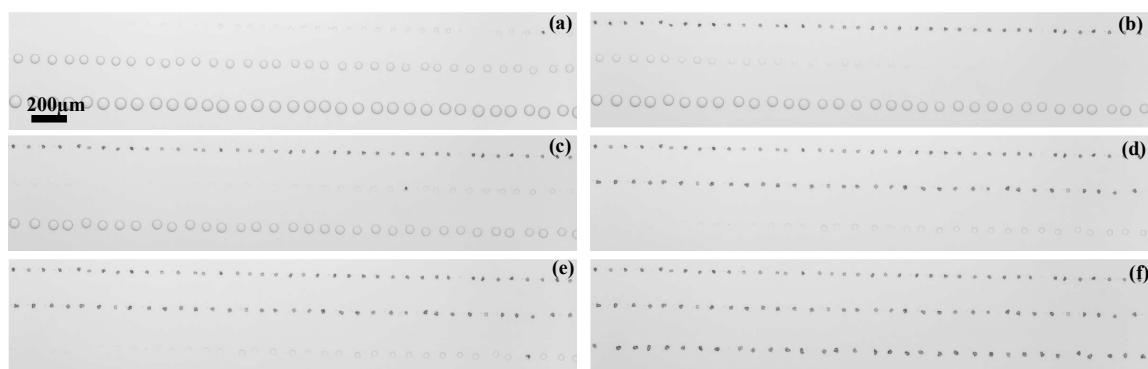


Fig. 4: Time sequence showing nucleation of NaCl crystals (a) at $t=1106s$, (b) $t=1305s$ and (c) $t=1390s$, (d) at $t=1563s$, (e) $t=1680s$ and (f) $t=1995s$. In (a), (c) and (e) the first microdroplet in L1, L2 and L3 has crystallized and in (b), (d) and (f) all microdroplets in L1, L2 and L3 have crystallized. All micrographs are at the same magnification. rows L1, L2 and L3 are from Fig.3.

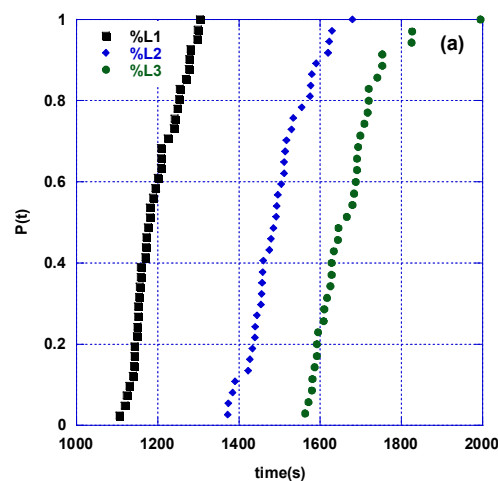


Fig. 5: Nucleation probability $P(t)$ vs time. $P(t)$ represent the normalized fraction of nucleated microdroplets. Rows L1, L2 and L3 are from Fig.3.

II. Direct Experiments

According to Davey et al.⁶³, “The biggest challenge is to identify the structure of low-concentration, nanosized dynamic clusters of molecules.” Thus, with the development of new experimental tools such as in-situ electron microscopy⁶⁴, cryogenic transmission electron microscopy^{65, 66}, fluctuation transmission electron microscopy⁶⁷, AFM⁶⁸, laser scanning confocal microscopy⁶⁹, laser confocal differential interference contrast microscopy⁷⁰ or even classical microscopy for colloidal nucleation⁷¹, increasing focus is placed on how to catch the critical cluster. The challenge is that nucleation is stochastic: during an experiment, we do not know where and when nucleation will occur. All we can do in our different laboratories for the moment is perform many experiments and hope that the law of the large numbers, will allow us to observe critical clusters. Whether or not this experimental observation is representative of the nucleation is still an open question (see the controversy over the existence of prenucleation aggregates).

II.1. Confinement by volume and external field.

Here, we address the unpredictability of the spatial and temporal location of the critical nucleus. In the experiment presented in Figs.3 and 4, confinement by volume allows us to have spatial control at the picoliter scale. With this set-up a resolution better than $1\mu\text{m}$ would be difficult to obtain, which is still far from the expected size of a critical cluster.

Thus, we propose confinement coupled to external field in order to control the location of the nucleation event. The implications of an external field for crystal growth in solution were highlighted by Voss⁷², Oxtoby⁷³ and Revalor⁵². Two effects on the supersaturated solutions are expected: molecular orientation and density fluctuation. The principle of the experiment is first generate solute microdroplets in oil with the microinjector and the microdroplets concentrate contraction to generate supersaturation. Second when the microdroplets completely disappears a sharp tip is used to induce a nucleation event by touching the supersaturated metastable microdroplet.

It was previously shown that any disturbance, for instance a crystal touching dense droplets⁷⁴ or mechanical contact with a nanotip⁷⁵, triggers nucleation. In the experiment presented in Fig.6, we induced a structural transformation via mechanical contact at precisely determined

points (at 16nm accuracy) and times, using an sCMOS camera at 200frames/s (ANDEOR NEO). The time between tip contact and observation of nucleation was shorter than 5ms (Fig.6a-b) and the mean crystal growth rate was greater than 200 $\mu\text{m/s}$ during the first 20ms (Fig.6a-c). Crystal nucleated was rough and transition to a faceted crystal was observed in less than 1s, i.e. the transition between the nucleation form and the equilibrium form. In practice, because the tip position is controlled with micromanipulators, the position of the critical nucleus can be determined with an accuracy of 16nm.

This method has some drawbacks, however. First, it is a trial and error method: the droplet is repeatedly tapped with the tip during the generation of supersaturation by water diffusion in order to launch nucleation. Second, it is less successful with protein, probably because the crystallization medium is not binary but ternary, that is to say composed of a solvent, a solute and crystallization agents. During droplet contraction both protein and crystallization agents concentrate and reach supersaturation. Then, for kinetic reasons⁷⁶, salt crystallizes first and/or polymer induces an LLPS, often before protein nucleation. For these reasons, we use another experimental procedure to generate supersaturation for protein crystallization experiments as described in the next section of the paper.

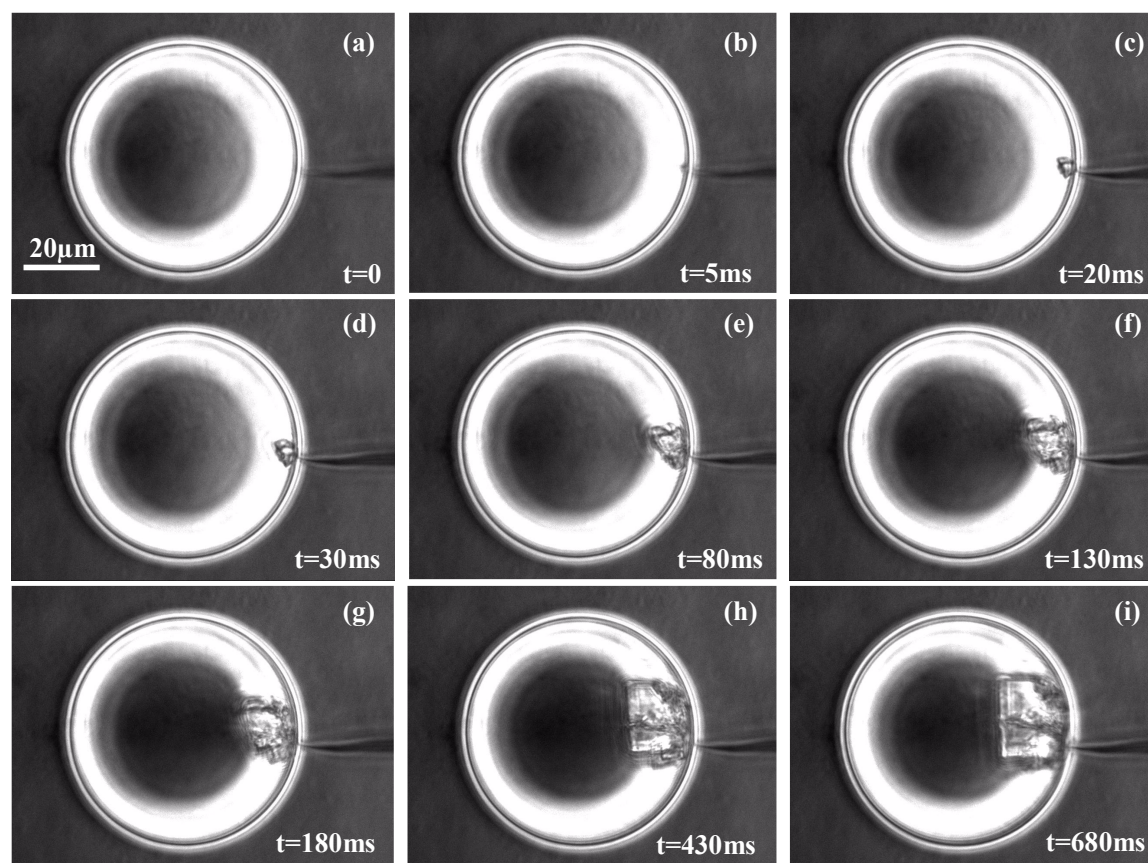


FIG.6: Panels represent time sequence showing nucleation induced by a sharp tip and growth of NaCl in paraffin oil. (a) initial condition: $\beta > 1.24$, (a) droplet size 60 μm (95pL assuming a spherical shape for the droplet with a contact angle of 120° at the time of nucleation as measured previously⁶¹). All micrographs (phase contrast mode) are at the same magnification.

II.2. Confinement by fluxes.

In this section, we describe how we use an external localized DC electric field to control the location of the nucleation event. Two electrodes were placed in a supersaturated metastable

lysozyme solution (Fig.7a), one of the electrodes being sharp (Fig.7b). Because of the nanometer size of the tip, large electric fields⁷⁷ and large field gradients are encountered near the tip at low DC voltage. This geometry also induces high current density inside the solution close to the region of high curvature. Here, supersaturation was increased by a flux and an accumulation of molecules at a precise point in the vicinity of the tip apex.⁴¹ This accumulation created inside the crystallization cell a concentration gradient that in solution is counteracted by convection. Therefore, the experiments were performed in gel in order to eliminate convection and keep the confinement in the vicinity of the electrode until concentration reaches the critical supersaturation.

The sequence presented in Fig. 8 shows that the use of gel as crystallization medium clearly enables better control of the location of nucleation and the nucleus appears in the vicinity of the cathode at the tip apex where the electric field is the strongest. As a result:

- (1) The nucleation time in presence of the DC electric field is shorter than 600s (instead of $t > 24$ h in absence of electric field); the nucleus is depicted by a circle in Fig. 8a.
- (2) The particle is rough, due to high local supersaturation encountered during nucleation and growth.
- (3) The average crystal growth rate (between 600 and 10800s) is $15\mu\text{m/h}$ in agreement with the growth rate obtained by Durbin et al.⁷⁸ at high supersaturation for lysozyme.
- (4) The current vs time curve during the experiment clearly shows a modification in the slope at 300s (Fig.9), just before the nucleation becomes optically observable in Fig.8a. Measuring current variation over time is thus a more sensitive way to detect nucleation than optical observation a better control is expected. A theoretical study of the field nano-localization with alternating voltage is in progress in our group⁷⁹, a better understanding of the effect of the localized electric field on nucleation is expected.

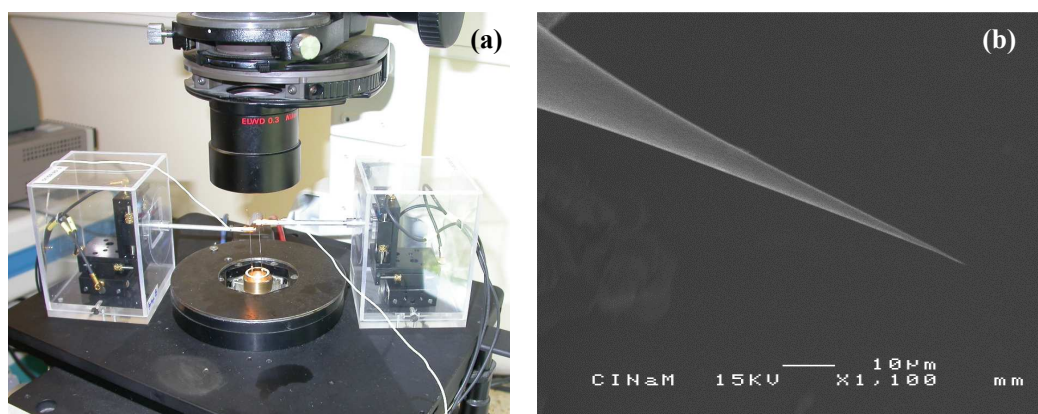


FIG.7: (a) temperature-controlled crystallization cell with the 2 micromanipulators and (b) SEM image of a W-tip.

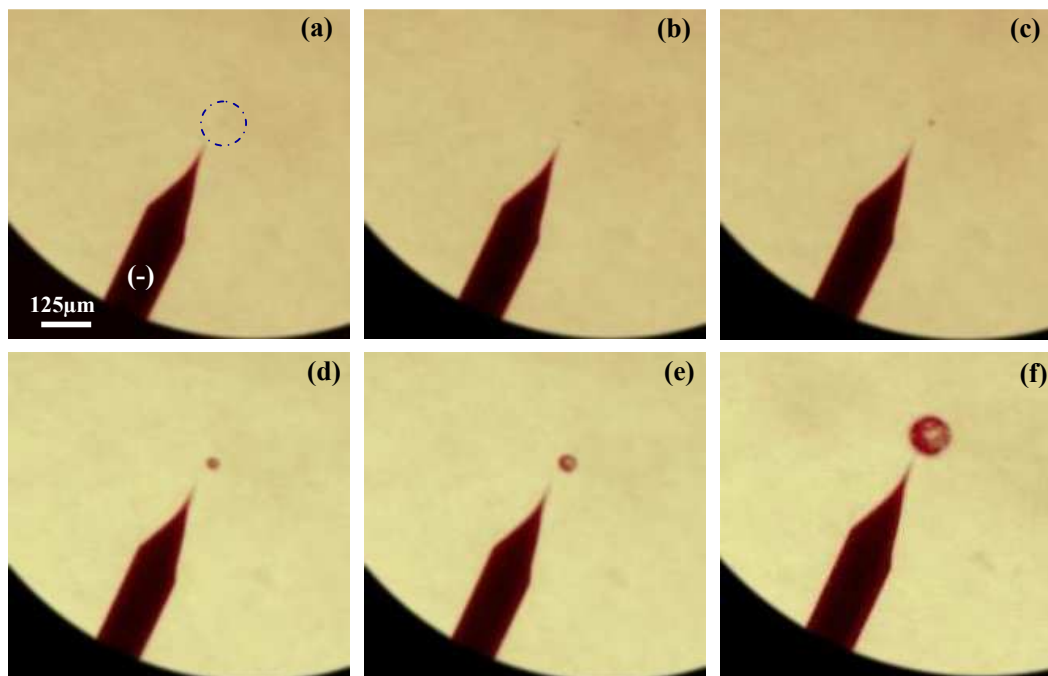


FIG.8: Panels represent time sequence showing nucleation and growth of lysozyme 20mg/ml NaCl 0.7M in agarose gel 1% (initial conditions: 0.5V- 0.35 μ A) at (a) $t=600$ s, (b) $t= 1200$ s, (c) $t=1800$ s, (d) $t=7200$ s, (e) $t=10800$ s and (f) $t=30000$ s. (The (-) indicates the anode).

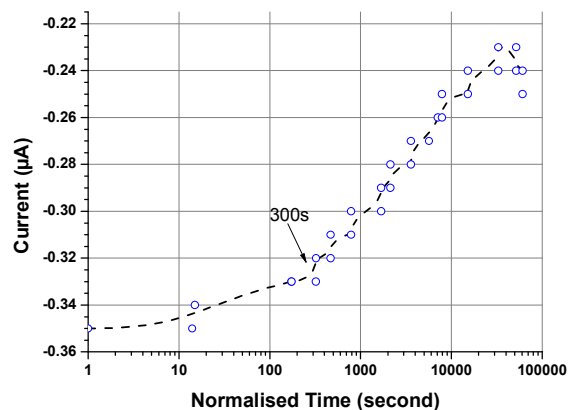


FIG.9: Evolution of the current over time during the experiment, semi-log scale. Line is a guide for the eye.

Conclusions

If all molecules follow the same rules⁸⁰ concerning crystallization, even though each material exhibits specific characteristics, the question is do they have different nucleation mechanisms, as frequently proposed in the literature?

In this paper, we present different experimental approaches to study and control nucleation. The use of small volumes makes it possible to measure nucleation kinetics. We also show that coupling volume reduction with use of an external field makes it possible to obtain spatial

and temporal control over nucleation for small molecules. Application to macromolecule raises some difficulties; however the use of an electric field to create localized field and fluxes shows promising results, leading to spatial control of nucleation. These experiments also shed light on some of the factors influencing the nucleation process.

Acknowledgements

We thank N. Ferté for protein characterization and fruitful discussions. We thank M. Sweetko for English revision.

References

1. Kashchiev D., *Nucleation : basic theory with applications*, Butterworth-Heinemann, Oxford, 2000.
2. J. Gibbs, *The Collected Works. Vol. I. Thermodynamics*, Yale University Press, 1948.
3. N. M. Dixit, A. M. Kulkarni and C. F. Zukoski, *Colloids and Surfaces A: Physicochemical and Engineering Aspects*, 2001, **190**, 47-60.
4. S. Selimovic, Y. Jia and S. Fraden, *Crystal Growth & Design*, 2009, **9**, 1806-1810.
5. M. Ildefonso, N. Candoni and S. Veessler, *Crystal Growth & Design*, 2013, **13**, 2107-2110.
6. Galkin O. and Vekilov P.G., *J. Phys. Chem. B.*, 1999, **103**, 10965-10971.
7. Galkin O. and Vekilov P.G., *J. Am. Chem. Soc.*, 2000, **122**, 156-163.
8. T. Azuma, K. Tsukamoto and I. Sunagawa, *J. Crystal Growth*, 1989, **98**, 371-376.
9. Georgalis Y., Zouni A. and Saenger W., *J. Crystal Growth*, 1992, **118**, 360-364.
10. Georgalis Y., Zouni A., Eberstein W. and Saenger W., *J. Crystal Growth*, 1993, **126**, 245-260.
11. Georgalis Y. and Saenger W., *Advances in Colloidal and Interface Sciences*, 1993, **46**, 165-183.
12. Boue F., Lefauchaux F., Robert M.C. and Rosenman I., *J. Crystal Growth*, 1993, **133**, 246-254.
13. Malkin A.J. and Mcpherson A., *Acta Cryst.*, 1994, **D50**, 385-395.
14. Niimura N., Minezaki Y., Ataka M. and Katsura T., *J. Crystal Growth*, 1994, **137**, 671-675.
15. Niimura N., Minezaki Y., Ataka M. and Katsura T., *J. Crystal Growth*, 1995, **154**, 136-144.
16. Niimura N., Ataka M., Minezaki Y. and Katsura T., *Elsevier Physica*, 1995, **B 213 et 214**, 745-747.
17. Minezaki Y., Niimura N., Ataka M. and Katsura T., *Biophysical Chemistry*, 1996, **58**, 355-363.
18. Niimura N., Minezaki Y., Tanaka I., Fujiwara S. and Ataka M., *J. Crystal Growth*, 1999, **200**, 265-270.
19. A. Stradner, H. Sedgwick, F. Cardinaux, W. Poon, C K., S. Egelhaaf, U, and P. Schurtenberger, *Nature*, 2004, **432**, 492-495.
20. Bishop J.B., Fredericks W.J., Howard S.B. and Sawada T., *J. Crystal Growth*, 1992, **122**, 41-49.
21. S. Veessler, S. Marcq, S. Lafont, J. P. Astier and R. Boistelle, *Acta Cryst*, 1994, **D50**, 355.
22. Muschol M. and Rosenberger F., *J. Crystal Growth*, 1996, **167**, 738-747.
23. F. Rosenberger, P. G. Vekilov, M. Muschol and B. R. Thomas, *Journal of Crystal Growth*, 1996, **168**, 1-27.
24. S. Finet, F. Bonnete, J. Frouin, K. Provost and A. Tardieu, *Eur. Biophys. J.*, 1998, **27**, 263-271.
25. M. Budayova-Spano, F. Bonnete, J. P. Astier and S. Veessler, *Journal of Crystal Growth*, 2002, **235**, 547-554.
26. A. Shukla, E. Mylonas, E. Di Cola, S. Finet, P. Timmins, T. Narayanan and D. I. Svergun, *Proceedings of the National Academy of Sciences*, 2008, **105**, 5075-5080.
27. F. Bonneté, N. Ferté, J. P. Astier and S. Veessler, *Journal de Physique IV*, 2004, **118**, 3-13.
28. Lekkerkerker H.N.W., *Physica*, 1997, **A 244**, 227-237.
29. P. R. Ten Wolde and D. Frenkel, *Science*, 1997, **277**, 1975-1978.
30. V. J. Anderson and H. N. W. Lekkerkerker, *Nature*, 2002, **416**, 811-815.
31. D. Gebauer and H. Cölfen, *Nano Today*, 2011, **6**, 564-584.
32. P. G. Vekilov, *Crystal Growth & Design*, 2004, **4**, 671-685.
33. D. Erdemir, A. Y. Lee and A. S. Myerson, *Accounts of Chemical Research*, 2009, **42**, 621-629.
34. D. Knezic, J. Zaccaro and A. S. Myerson, *The Journal of Physical Chemistry B*, 2004, **108**, 10672-10677.
35. R. P. Sear, *CrystEngComm*, 2014, **16**, 6506-6522.

36. R. D. Dombrowski, J. D. Litster, N. J. Wagner and Y. He, *Chemical Engineering Science*, 2007, **62**, 4802-4810.
37. M. Ildefonso, N. Candoni and S. Veessler, *Organic Process Research & Development*, 2012, **16**, 556-560.
38. Grossier R., Hammadi Z., Morin R., Magnaldo A. and Veessler S, *Applied Physics Letters*, 2011, **98**, 091916-091913.
39. E. W. Muller and T. T. Tsong, *Field ion microscopy : principles and applications*, American Elsevier Publishing Company, New York, 1969.
40. Z. Hammadi, M. Gauch and R. Morin, *Journal of Vacuum Science & Technology B: Microelectronics and Nanometer Structures*, 1999, **17**, 1390-1394.
41. Z. Hammadi, J. P. Astier, R. Morin and S. Veessler, *Crystal Growth & Design*, 2007, **7**, 1476-1482.
42. M. C. Robert and F. Lefauchaux, *Journal of Crystal Growth*, 1988, **90**, 358-367.
43. S. Lee and J. Wiener, *Journal of Chemical Education*, 2010, **88**, 151-157.
44. Ildefonso M., Candoni N. and Veessler S., *Cryst. Growth Des.*, 2011, **11**, 1527-1530.
45. Grossier R. and Veessler S., *Cryst. Growth Des.*, 2009, **9**, 1917-1922.
46. Z. Kozisek, K. Sato, S. Ueno and P. Demo, *The Journal of Chemical Physics*, 2011, **134**, 094508-094509.
47. D. Kashchiev, *The Journal of Chemical Physics*, 2011, **134**, 196102-196102.
48. P. Laval, J.-B. Salmon and M. Joanicot, *Journal of Crystal Growth*, 2007, **303**, 622-628.
49. L. Goh, K. Chen, V. Bhamidi, G. He, N. C. S. Kee, P. J. A. Kenis, C. F. Zukoski and R. D. Braatz, *Crystal Growth & Design*, 2010, **10**, 2515-2521.
50. S. V. Akella, A. Mowitz, M. Heymann and S. Fraden, *Crystal Growth & Design*, 2014, **14**, 4487-4509.
51. D. Tsekova, S. Dimitrova and C. N. Naneev, *Journal of Crystal Growth*, 1999, **196**, 226-233.
52. Revalor E., Hammadi Z., Astier J. P., Grossier R., Garcia E., Hoff C., Furuta K., Okutsu T., Morin R. and Veessler S, *J. Crystal Growth*, 2010, **312**, 939-946.
53. P. B. Duncan and D. Needham, *Langmuir*, 2006, **22**, 4190-4197.
54. K. Allain, R. Bebawee and S. Lee, *Crystal Growth & Design*, 2009, **9**, 3183-3190.
55. Bempah O. A. and Hileman Jr. O. E., *Can. J. Chem.*, 1973, **51**, 3435-3442.
56. Ha J.-M., Wolf J. H., Hillmyer M. A. and Ward M. D., *Journal of American Chemical Society*, 2004, **126**, 3382-3383.
57. M. Beiner, G. T. Rengarajan, S. Pankaj, D. Enke and M. Steinhart, *Nano Letters*, 2007, **7**, 1381-1385.
58. K. Kim, I. S. Lee, A. Centrone, T. A. Hatton and A. S. Myerson, *Journal of the American Chemical Society*, 2009, **131**, 18212-18213.
59. C. J. Stephens, S. F. Ladden, F. C. Meldrum and H. K. Christenson, *Advanced Functional Materials*, 2010, **20**, 2108-2115.
60. Grossier R., Magnaldo A. and Veessler S, *J. Crystal Growth*, 2010, **312**, 487-489.
61. I. Rodríguez-Ruiz, Z. Hammadi, R. Grossier, J. Gómez-Morales and S. Veessler, *Langmuir*, 2013, **29**, 12628-12632.
62. H. Langer and H. Offermann, *Journal of Crystal Growth*, 1982, **60**, 389-392.
63. R. J. Davey, S. L. M. Schroeder and J. H. Ter Horst, *Angewandte Chemie International Edition*, 2013, **52**, 2166-2179.
64. Y. Kimura, H. Niinomi, K. Tsukamoto and J. M. García-Ruiz, *Journal of the American Chemical Society*, 2014, **136**, 1762-1765.
65. E. M. Pouget, P. H. H. Bomans, J. a. C. M. Goos, P. M. Frederik, G. De With and N. a. J. M. Sommerdijk, *Science*, 2009, **323**, 1455-1458.
66. J. Baumgartner, A. Dey, P. H. H. Bomans, C. Le Coadou, P. Fratzl, N. a. J. M. Sommerdijk and D. Faivre, *Nat Mater*, 2013, **12**, 310-314.
67. B.-S. Lee, G. W. Burr, R. M. Shelby, S. Raoux, C. T. Rettner, S. N. Bogle, K. Darmawikarta, S. G. Bishop and J. R. Abelson, *Science*, 2009, **326**, 980-984.

68. S. T. Yau and P. G. Vekilov, *Nature*, 2000, **406**, 494-497.
69. U. Gasser, E. R. Weeks, A. Schofield, P. N. Pusey and D. A. Weitz, *Science*, 2001, **292**, 258-262.
70. M. Sleutel and A. E. S. Van Driessche, *Proceedings of the National Academy of Sciences*, 2014, **111**, E546-E553.
71. Zhang K. -Q. and Liu X. Y., *Nature*, 2004, **429**, 739-743.
72. D. Voss, *Science*, 1996, **274**, 1325.
73. D. W. Oxtoby, *Nature*, 2002, **420**, 277-278.
74. D. Vivares, E. W. Kalera and A. M. Lenhoff, *Acta Crystallographica Section D*, 2005, **61**, 819-825.
75. R. Grossier, Z. Hammadi, R. Morin and S. Veessler, *Physical Review Letters*, 2011, **107**, 025504.
76. A. A. Chernov, *Physics Reports I.M. Lifshitz and Condensed Matter Theory*, 1997, **288**, 61-75.
77. Gomer R., *Field emission and field ionization*, Harvard University press, Cambridge, 1961.
78. Durbin S.D. and Feher G., *J. Crystal Growth*, 1986, **76**, 583-592.
79. Z. Hammadi, R. Morin and J. Olives, *Applied Physics Letters*, 2013, **103**, 223106.
80. Chernov A.A. , *Journal of Materials Science: Materials in Electronics*, 2001, **12**, 437-449.